KIMIKA Volume 35, Number 1, pp. 45-61 (2024)
 ISSN 2508-0911
https://doi.org/10.26534/kimika.v35i1.45-61

Synthesis of BSA-stabilized copper nanoclusters and evaluation of their potential use as fluorescent sensors for folic acid

Krysma Irene R. Munar, Maritess M. Lacquio, Bong Carlo N. Remillon, Mariam C. Recuenco*

Institute of Chemistry, College of Arts and Sciences, University of the Philippines Los Baños, Brgy. Batong Malake, Los Baños, Laguna 4031, Philippines

*Author to whom correspondence should be addressed; email: mcrecuenco@up.edu.ph

ABSTRACT

This study describes the synthesis and characterization of BSA-stabilized copper nanoclusters (BSA-CuNCs) for use as sensors for the B vitamin folic acid. Ascorbate served as a reducing agent while bovine serum albumin (BSA) served as a capping and stabilizing agent. The BSA-CuNCs had a golden-yellow appearance and perceivably have good dispersibility. Transmission electron microscopy indicated average diameters of the BSA-CuNCs as 2.47 ± 0.50 nm. With atomic force microscopy and dynamic light scattering, the diameters of the BSA-CuNCs were varied and larger than anticipated (64 ± 13 nm AFM; 11-608 nm DLS), since nanocluster sizes should be less than 2 nm. The BSA-CuNCs' UV–visible spectra did not show peaks in the 500–600 nm indicating the absence of the surface plasmon resonance (SPR) of larger nanoparticles. The BSA-CuNCs were excited at 320 nm and showed a fluorescence emission at 644 nm. The BSA-CuNCs were then evaluated as potential folic acid sensors. Fluorescence quenching was observed as folic acid was added incrementally. The quenching fitted well with the Stern-Volmer equation, with estimated limits for detection (LOD) and quantitation (LOQ) at 0.77 μg/mL and 2.35 μg/mL, respectively. Next, the folic acid content of some over-the-counter supplements was assessed. There was a range of 33.31% to 40.21% in the percent error between the claimed and experimental folic acid values, which were beyond the acceptable accuracy and precision errors of 5% and 10%, respectively. Nevertheless, current results may suggest potential that the BSA-CuNCs may be used to quantify folic acid. However, further research is required to improve sample preparations and analytical procedures.

Keywords: *folic acid, copper nanoclusters, bovine serum albumin, fluorescence quenching, Stern-Volmer equation*

INTRODUCTION

Metal nanoclusters with sizes near the Fermi wavelength of electrons bridge the gap between metal atoms and metal nanoparticle behaviors (Zheng et al., 2004). Because of their small size, they have distinct size-dependent characteristics, such as molecule-like and fluorescent properties (Qu et al., 2015). Gold and silver nanoclusters have received the most attention of any metal nanoclusters previously studied (Zhao et al., 2015). Applications for gold and silver-based metal nanoclusters include biosensing, biolabeling, and bioimaging (Wang et al., 2017). They were reportedly better at biological labeling and sensing because of their small size. Advantages also include biocompatibility, increased tracking lifetime, sensitivity, and stability. Furthermore, metal nanoclusters are more likely to be less toxic than conventional fluorophores (Ou et al., 2018).

Recently, there has been much interest in the use of copper-based nanostructures in a variety of fields, including catalysis, electronics, water purification, agriculture, and medicine, to function as an alternative to commonly used but more costly metals like gold and silver (Jardon-Maximino, 2018). Copper nanoclusters with a core size of less than 2 nm are among the copper-based nanostructures that could be prepared for various applications.

Zheng et al. (2004) stated that nanoclusters have unique characteristics when their size is less than 3 nm. When distinguishing nanoclusters from larger nanoparticles, the most frequently used parameter is the lack of surface plasmon resonance (SPR). There is a peak in the absorption spectrum observed at approximately 500–600 nm for larger metal nanoparticles; however, since metal nanoclusters are too small to sustain surface plasmon resonance, the peak cannot exist (Xu and Han, 2016).

The fluorescence of nanoclusters is another fascinating characteristic. When a sample is exposed to light at a specific wavelength, an electron is excited to a higher energy level, relaxes into a lower energy state, and eventually returns to its ground state. This process is known as fluorescence. The final phase enables photon formation and light emission from the fluorescent sample (Selegard, 2013). The energy level spacing and free electronic density significantly impact the HOMO-LUMO transitions and the transition energy. Size affects the energy level spacing. Free electrons behave in discrete energy levels, and as the radius of the nanoparticle decreases, the energy level spacing increases (Qu et al., 2015). Furthermore, the fluorescence property may be influenced by any ligands that may be attached to the nanoparticle (Qu et al., 2015).

The synthesis of copper nanoclusters is quite challenging because of their instability in aqueous solutions and sensitivity to air, which may cause surface oxidation (Xiaoqing et al., 2015). Several capping agents were investigated as useful stabilizers to help prevent nanocluster aggregation and address this problem (Zhao et al., 2015). An appropriate capping agent requires an amphiphilic molecule with a nonpolar tail that can interact with the environment and a polar head with functional groups with donor atoms that can coordinate with the metal atoms or ions.

This work synthesized the copper nanoclusters using bovine serum albumin as a stabilizing agent. The synthesis of protein-stabilized gold nanoclusters using bovine serum albumin was first reported by Xie et al. (2009). In its native form, bovine serum albumin (BSA) is a heart-shaped protein with three homologous domains that each contain ionizable groups (Au et al., 2010). Because it contains scaffolds, pockets, and multiple accessible functional groups that can coordinate with metal atoms, BSA can be a helpful stabilizing agent in synthesizing nanoclusters (Jose et al., 2015). According to Singh et al. (2005), its zwitterionic characteristic and exposed ionic groups make it ideal for cationic and anionic binding.

Reduction can occur when the stabilizing or capping agent used in synthesizing nanoclusters has sufficient reducing power. Nevertheless, synthesizing the nanoclusters takes long when the

stabilizing agents' reducing effect is weak. Therefore, reducing agents are usually added to speed up the reaction. Sodium borohydride and sodium hydroxide were the most often used reducing agents in the synthesis of nanoclusters. However, some of the bio-analytical applications of the nanoclusters may be significantly affected by these reducing agents due to their relative toxicity (Lerma-Garcia et al., 2014). Therefore, finding reducing agents that can minimize these complications while being comparatively safer and environmentally friendly is very important.

The water-soluble vitamin C plays several physiological roles, including tyrosine metabolism, collagen synthesis, carnitine synthesis, dopamine conversion to norepinephrine, and peptide amidation (Hacisevki, 2009). It is also well known that ascorbic acid, which oxidizes to dehydroascorbic acid during the redox reaction, is a good reducing agent and can be used for metal nanoparticle synthesis.

Pteroylmonoglutamic acid, or folic acid, is a crucial nutrient that should be taken by pregnant women, in particular to prevent neural tube defects. An embryonic tube's abnormal closure causes neural tube defects (NTDs), which seriously impede a child's ability to develop physically and mentally. According to Santos et al. (2016), NTDs can be divided into two categories: those that affect the brain, like anencephaly, and those that affect the spinal cord, like spina bifida. NTD-affected pregnancies can result in stillbirth, miscarriage, or a live birth with complications (Blencowe et al., 2018). Every year, about 300,000 babies are born with it worldwide, making it the most common cause of neonatal morbidity and mortality.

The term "folate" is applied to the naturally occurring form of Vitamin B9, while "folic acid" is applied to the synthetic form. There is a need to determine folate/folic acid content in foods and dietary supplements, and in human biological samples such as blood and urine. Due to the vitamin's roles in growth and development, nutritional deficiencies must be prevented. Thus, public health policies indicate recommendations for folate/folic acid intake and supplementation (Field and Stover, 2018). In addition, there are some regulations regarding food processing and fortification, quality control and labelling (Field and Stover, 2018). According to Quinlivan et al. (2096), the most popular techniques for analyzing folic acid and folates are potentiometric, colorimetric, spectroscopic, and high-pressure liquid chromatography (HPLC), which uses various detectors, mobile phases, and columns. Unfortunately, most of these techniques call for the use of organic solvents, which present hazards to the environment and human health. Others use microbiological assays to measure folates and folic acid based on the growth response of bacteria, typically *Lactobacillus casei*, which has been shown to respond primarily to various folate derivatives (Rahman et al., 2015). Nonetheless, microbiological assays required a laborious and meticulous procedure.

A number of studies had reported that the copper nanoclusters may be potential sensors due to the observed changes, either quenching or enhancement, in their fluorescent properties in the presence of different substances (Aparna et al., 2019). Such changes were observed to be dependent on the concentration of the analyte. Fluorescence quenching seems to be the more common response in the presence of the analyte. For protein-stabilized nanoclusters, fluorescence quenching may be due to the binding of the added analyte to the protein, which results in conformational changes (Umavedi, 2017). For nanoparticles measuring less than 5 nm, fluorescence quenching may be due to an electron transfer (Umavedi, 2017). For nanoparticles greater than 5 nm, energy transfer may be the more predominant mechanism (Umavedi, 2017). In the fluorescence quenching of gold nanoclusters by dopamine, the nanocluster may have formed electron-hole pairs, which may have readily reacted with the acidic dopamine protons (Govindaraju et al., 2017). The electron hole could have been filled from an electron transfer from dopamine. However, there is still a lack of knowledge on the exact mechanism of the fluorescence and quenching properties of protein coated metal nanoclusters primarily due to the inherent complexities of protein templates and lack of structural information on the nanoclusters. (Hemmateenejad et al., 2014).

This study investigated the potential use of copper nanoclusters as folic acid biosensors to develop a simple yet sensitive and safer alternative to conventional folic acid analysis. The proposed method is based on the fluorescence quenching of the BSA-stabilized copper nanoclusters in the presence of folic acid.

METHODS

Synthesis of Bovine Serum Albumin-Stabilized Nanoclusters (BSA-CuNCs). The synthesis procedure was adapted and modified from Zhao et al. (2015). BSA was obtained from Sigma-Aldrich (A7906), while $CuSO_4 \cdot 5H_2O$ was from JT Baker. In a screw-capped container, 2 mL of 20 mM solution of $CuSO_4$ was added to 10 mL of 10 mg/mL solution of BSA. The blue viscous paste was stirred vigorously on a magnetic stirrer for about 2 minutes. Then, the pH of the paste was adjusted to pH 12 by carefully adding 1 M NaOH solution. Subsequently, 1 mL of freshly prepared 1 M ascorbic acid solution was added to the solution and stirred vigorously for 5 minutes. The resulting solution was incubated and undisturbed at room temperature for 24 hours. The product was stored in the refrigerator at around 4 ^{o}C until further use.

Characterization of BSA-CuNCs. The UV-visible spectrum of the BSA-CuNCs were obtained using Shimadzu UV Mini 1240. Particle sizes were determined using dynamic light scattering (DLS) zetasizer (Malvern Instruments Zeta Sizer Nano ZS90) and atomic force microscopy (AFM) (Park Systems XE-70 AFM with XEI Software for image analysis) through the UPLB Nanoscience and Technology Facility Analytical and Instrumentation Service Laboratory. Transmission electron microscope images were obtained using the Hitachi H-7000 TEM at Kobe University, Department of Electrical and Electronic Engineering. Particle sizes were estimated using the ImageJ software.

General Procedure for Fluorescence Quenching Assay. In a 3 mL cuvette, 300 µL of BSA-CuNCs were mixed with 2700 µL of distilled water. The fluorescence intensity (F_0) at 644 nm of the dilute solution upon excitation at 320 nm was measured using Shimadzu RF-5301 PC. Then, 2 µL of standard solution/sample was added, and its new fluorescence intensity (F) was again measured.

Construction of Calibration Curve and Analytical Figures of Merit. The calibration curve was constructed by plotting the fluorescence quenching ratio (F_o/F) against folic acid concentration (0, 0.67, 1.33, 2.00, 2.66, 3.32, 3.98, 4.64, 5.31, and 5.96 µg/mL) which was based on the simplest case of Stern-Volmer equation which describes the kinetics of fluorescence quenching,

$$\frac{F_0}{F} = 1 + K_{sv}\,[Q]$$

Where $\frac{F_0}{F}$ is the fluorescence quenching ratio, K_{sv} is the Stern-Volmer constant, and [Q] is the concentration of the quencher. The values plotted for the final calibration curve were the average of three calibration curves constructed. From the final calibration curve, the limit of detection (LOD) and limit of quantification (LOQ) were determined using the following equations:

$$\text{LOD} = 3.3\ s/S$$

$$\text{LOQ} = 10\ s/S$$

Where s is the standard deviation of the intercept of the regression line, and S is the slope of the calibration curve. The fluorescence quenching ratio for the LOQ was determined by interpolation using the calibration curve.

Preparation of Supplement Samples for Folic Acid (FA) Analysis. Different brands of folic acid supplements were used to test the BSA-CuNCs as sensors for the analysis of folic acid. One tablet from each supplement was finely ground using mortar and pestle and was dissolved in 500 µL of 0.1 M NaOH solution. Then, the resulting solution was filtered using ashless Whatman No. 40 filter paper. The filtrate was collected, diluted to 100 mL, and transferred to polyethylene (PE) bottles.

***Fluorometric Determination of Folic Acid*.** The fluorescence quenching ratios for the four samples were determined using the general procedure for fluorescence quenching assay. Appropriate dilutions were prepared. Twelve trials for each supplement were performed. The experimental concentrations were determined through interpolation in the working range obtained from the calibration curve and LOQ.

The percent mean recovery and relative standard deviations were calculated using the following equations:

$$\% \text{ Mean Recovery} = \frac{Experimental\ concentration}{Concentration,\ \ manufacturer's\ claim} \text{ x } 100\%$$

$$\% \text{ Error} = \frac{FA\ Declared - FA\ Experimental}{FA\ Declared} \text{ x } 100\%$$

Outliers in the experimental results were determined statistically using Dixon's Q-test for single outliers and are calculated as follows:

$$Q_{exp} = \frac{X_2 - X_1}{X_n - X_1}$$

where X_2 is the suspect value, X_1 is the nearest value from the suspect value, X_n is the largest value, and X_1 is the lowest value. At a confidence level of 95 %, Q_{exp} was compared to Q_{crit} value of 0.426 since twelve replicates for each supplement brand were obtained. A Q_{exp} higher than Q_{crit} means the suspect value was an outlier.

RESULTS AND DISCUSSION

Synthesis of BSA Stabilized Copper Nanoclusters (BSA-CuNCs). Figure 1A shows the bottom-up approach to the preparation of BSA-CuNCs. The synthesis was performed in a sealed container to minimize the presence of air and decrease the chances of copper oxidation. A viscous blue paste was formed after adding $CuSO_4$ solution to the BSA solution. In this step, a Cu^{2+}-BSA$^-$ ion-association formed from the electrostatic interaction between Cu^{2+} and the negatively charged BSA that was due to the dissociation of its free carboxyl groups in the neutral aqueous solution. The water solubility of the protein in the ion association was improved by adjusting the pH to pH 12 by adding 1 M NaOH. The viscous blue paste was transformed into a purple transparent solution. This step exposed free amino groups to combine with Cu^{2+} in forming a stable BSA-Cu complex (Xiaoqing et al., 2015).

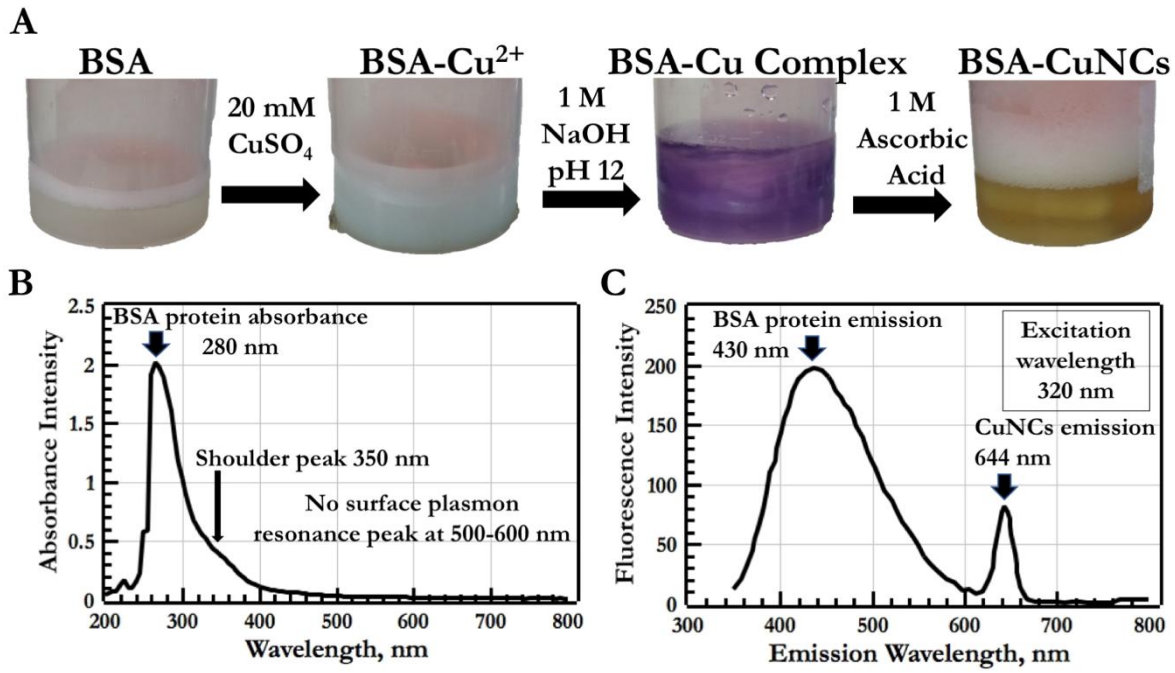

Figure 1. Synthesis and characterization of BSA stabilized copper nanoclusters (BSA-CuNCs). A. BSA solution (10 mg/mL) and 20 mM CuSO4 formed a viscous mixture. Adjusting to pH 12 allowed the formation of the violet BSA-Cu complex solution. The addition of ascorbic acid initiates the reduction of copper to synthesize BSA-CuNCs. B. The UV-visible absorption spectrum of BSA-CuNCs. The strong peak at ~280 nm is due to the BSA protein. A tiny shoulder peak at around ~350 nm suggests a molecular-like optical absorption of CuNCs. No peak at ~500-600 nm indicated the absence of surface plasmon resonance (SPR). The absence of a peak at ~800 nm indicates that a copper oxide monolayer was not present. C. The emission spectrum of BSA-CuNCs shows a peak at 430 nm likely due to BSA, and a peak at 644 nm due to the copper nanoclusters.

In the synthesis, BSA acted as a stabilizing and mild reducing agent. The globular protein having 583 residues, including 17 cysteine residues for disulfide linkages, has only one free thiol group that may act as a reducing agent. The protein also has 40 tyrosine residues which may contribute to its reducing property (Au et al., 2010). A high ratio of BSA to copper ions was used for stabilizing the nanoclusters.

An alkaline pH was used to possibly effect the cleavage of the disulfide bonds in BSA to expose free thiol groups. The thiol groups could react with Cu^{2+} to form Cu-S bonds thus providing steric protection on the nanoclusters. These would possibly create a BSA layer on the surface of the CuNCs for stability by preventing the oxidation of the copper atoms in the air (Xiaoqing et al., 2015).

The role of ascorbic acid in the synthesis was to reduce the time of reduction Cu^{2+} ions to Cu^{0}. Ascorbate donates protons and one to two electrons in the reaction. Moreover, ascorbic acid may also have added a stabilizing effect in the formation of nanoclusters by serving as capping agents or in the formation of a Cu-ascorbate complex (Xiong et al., 2011). Ascorbic acid, which has the ability to scavenge free radicals and reactive oxygen molecules, may also serve as an antioxidant to prevent or slow down the oxidation of copper (Jain et al., 2015).

The stirring of the synthesis mixture was set for about five minutes or until a pale-yellow solution was observed. Longer stirring times were avoided since it turned the pale-yellow solution to color orange to brown with no observed fluorescence emission.

Room temperature during the synthesis was chosen to maintain the interactions of the nanoclusters with BSA which may affect its stabilizing and capping effect. High temperatures may disrupt such interactions and may also induce the oxidation of copper. It was observed that disturbing the solution just right after the synthesis procedure would cause aggregation since precipitates were formed. Hence, the solution was incubated for 24 hours at room temperature (~25 ^{0}C) without any disturbance. After incubation, the pale-yellow solution turned golden yellow with perceivably good dispersibility, indicating the formation of the copper nanoclusters. The solution was stored in the refrigerator (~ 4^{0}C) in the dark until further use.

Optical Properties of BSA-CuNCs. The synthesized nanoclusters were characterized using UV-visible spectroscopy to investigate the presence of surface plasmon resonance using a spectrofluorophotometer to determine its fluorescence properties and dynamic light scattering and atomic force microscopy to determine its size, shape, and have an image of its topography.

Figure 1B shows the characteristics of the UV-visible absorption of the BSA-CuNCs. A peak due to surface plasmon resonance (SPR) around 500 nm to 600 nm was not observed, which indicates the successful synthesis of the BSA-CuNCs. The small sizes of nanoclusters could not support the formation of surface plasmon resonance. The absorbance at 280 nm was maximum absorption for BSA. A tiny shoulder peak at around ~350 nm suggests a molecular-like optical absorption of CuNCs due to the quantum confinement effect (Chen et al., 2018). The quantum confinement theory is when the electrons in the conduction band and the holes in the valence band are being confined spatially by a potential well, resulting in the increase in energy of the lowest energy optical transition from the valence to the conduction band (Sun, 2006). As the size of the nanostructure decreases, the band gap increases and the average energy of the electrons in the conduction band also increases. There was no absorption peak at around 800 nm which indicates that the copper oxide monolayer that may have formed due to oxidation of the copper was not present (Pacioni et al., 2013).

Figure 1C shows the two fluorescence emission wavelengths, at 430 nm and 644 nm, of the BSA-CuNCs upon excitation at 320 nm. Other excitation wavelengths such as 300 nm, 337 nm, 350 nm, and 370 nm, and with different combinations of slit widths were also used to determine the optimum excitation wavelength of the synthesized BSA-CuNCs. It was observed that the fluorescence emission was tunable at these wavelengths. Among all the excitation wavelengths used, it was at 320 nm, which showed the highest fluorescence intensity between 600-700 nm. Hence, 320 nm was chosen as the optimum excitation wavelength and was used throughout the experiment. The fluorescence seen at 430 nm may be from BSA from the fluorescence of aromatic amino acids, tryptophan, phenylalanine, and tyrosine (Teale et al., 1957). The emission at 644 nm was due to the CuNCs, thus the intensity at this wavelength was monitored during the addition of folic acid.

Size Analysis of BSA-CuNCs. Figure 2A shows the histogram of the particle size distribution of the synthesized BSA-CuNCs using dynamic light scattering (DLS) zetasizer. The results showed that several sizes of the BSA-CuNCs were generated. Based on the histogram, the sizes ranged from as small as around seven nanometers to as large as greater than 1000 nm.

The synthesized nanoclusters have sizes ranging from 11 nm to 608 nm with size average of 177 nm ± 25 nm in diameter. In addition, the DLS analysis indicated a high polydispersity of 0.735 for the sample. In DLS measurements, values greater than 0.7 indicate that there was a very broad size distribution, and the technique may not be suitable to use for the size analysis of the sample (Malvern Instruments Limited, 2011). The sizes generated from DLS were too large than the anticipated size, which was at most 2 nm.

Figures 2B and 2C show topographic images of the BSA-CuNCs using atomic force microscopy (AFM). These images suggest that the shape of the synthesized BSA-CuNCs was spherical with

average sizes of 63.90 nm ± 13.44 nm in diameter. The estimated sizes were also too large in comparison to the anticipated size of the nanoclusters. While AFM is commonly used for size estimation of nanoparticles, it seems that it might be beyond in its capabilities in analyzing nanoclusters at sizes of less than 2 nm. Artifacts and distortions could affect the quality of results obtained.

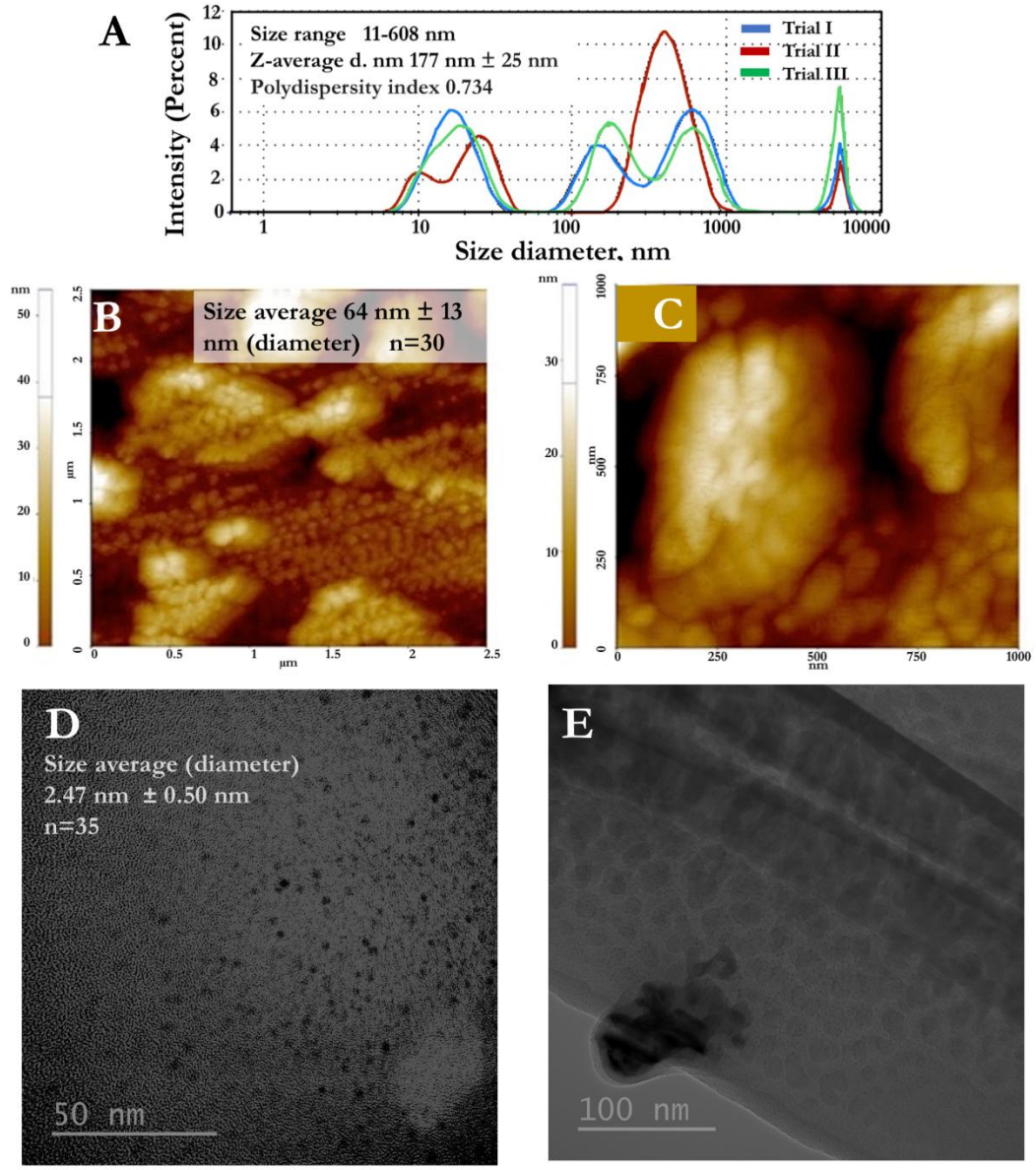

Figure 2. Size analysis of the BSA stabilized copper nanoclusters. A. Results of the dynamic light scattering indicated particles of average sizes of 177 nm ± 25 nm. B and C. Topographic images of the BSA stabilized copper nanoclusters using atomic force microscopy. Size average is 63.90 nm ± 13.44 nm in diameter. D and E. Transmission electron micrograph of BSA stabilized copper nanoclusters. Size average is 2.47 nm ± 0.50 nm in diameter.

Ultrasonication is routinely used for fragmentation of aggregates and to homogenize nanoparticle dispersions (Gokce et al., 2014, Glaubitz et al., 2022). Nguyen et al. (2011) demonstrated that ultrasonication reduced the size of alumina nanoscale particles from large aggregates (~5000

nm) into smaller clusters (<150 nm) using DLS and TEM. However, the study observed partial reaggregation at higher amplitudes (60%) or prolonged ultrasonication. Gocke et al. (2014) study showed that ultrasonication for 15 to 20 minutes effectively reduced the size of chitosan nanoparticles, but observed reheating and agglomeration with prolonged sonication. In this study, sonication was done prior to DLS, AFM and TEM analyses. However, as seen in the DLS and AFM results, sonication parameters used were not effective in decreasing agglomeration, and may favor reaggregation of copper nanoclusters, thus the polydispersity data observed in DLS. Ultrasonication may be an effective method for reducing particle size and achieving narrow distributions, but optimal conditions must be maintained to avoid reagglomeration (Gocke et al. 2014, Glaubitz et al., 2022).

The relatively large particle sizes obtained from both DLS and AFM may be due to possible aggregation or possible oxidation of the BSA-CuNCs. Copper nanoparticles were reported to be easily oxidized to form copper oxides (Ghorbani, 2015). We did not perform experiments to verify the formation of copper oxides, but this may be possible since copper oxides were reportedly more thermodynamically stable than copper metal nanoparticles (Rajesh et al., 2016). This may somehow depict the poor stability of the synthesized copper nanoclusters through time.

Transmission electron microscopy (TEM) would be the more appropriate technique for the BSA-CuNCs' size analysis. In our TEM analysis of the BSA- CuNCs, the size average obtained is 2.47 nm ± 0.50 nm in diameter (Figures 2D and 2E). These diameters agree with the typical sizes for nanoclusters. Based on our experience, even with the use of a TEM, it was challenging to visualize the BSA- CuNCs. At first, it appeared that the TEM images (100 nm and 50 nm scales) only showed more of the protein particles and aggregates. Upon closer inspection, the BSA- CuNCs could be seen as distinct dots and specks in the images.

Fluorometric Determination of Folic Acid. Figure 3A shows that as the concentration of folic acid added to BSA-CuNCs increases, the intensity of fluorescence at 644 nm decreases. Several reasons can be enumerated for how the fluorescence of the BSA-CuNCs was quenched when folic acid was added. The most common mechanisms may be due to the formation of different complexes. One is the formation of a ground state non-fluorescent complex in static quenching (Mohd et al., 2010). Another could be due to a collision followed by the formation of a complex between the nanocluster or fluorophore in excited state and quencher in the ground state in dynamic quenching. It may also be a combination of the two processes (Mohd et al., 2010).

Aparna et al. (2019) proposed a model of the BSA-CuNCs where copper nanoclusters are interspersed in the partly unfolded molecules of BSA. Aggregation of the CuNCs could have been prevented since portions of the peptide would surround the CuNCs. Quenching of the CuNCs' fluorescence in the presence of folic acid could be attributed to several possible interactions. Folic acid may interact with the CuNCs through Van der Waals forces. These interactions may result to static, dynamic or energy transfer modes of quenching. The BSA coating the CuNCs may also interact with folic acid through its peptide bonds and amino acid side chains via hydrogen bonding, electrostatic and hydrophobic interactions. Such interactions may result to shedding of the peptide coating, resulting to reduction of fluorescence of the CuNCs. Aggregation and/or oxidation may result from the loss of the peptide coat on the CuNCs. Another possibility is the formation of an electron hole in the CuNCs upon excitation followed by proton loss and electron transfer from folic acid resulting to the fluorescence quenching (Govindaraju et al., 2017). However, determining the mechanism of quenching was beyond the scope of this study. Hence, future works should consider determining the mechanism of quenching between the fluorescent BSA-CuNCs and folic acid. With the observed fluorescence quenching of the BSA-CuNCs, it was hypothesized that the BSA-CuNCs can be used as a biosensor for folic acid.

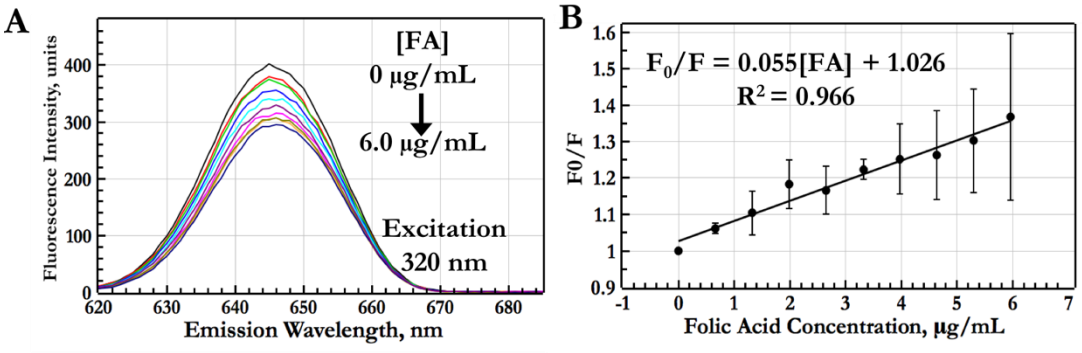

Figure 3. Fluorescence quenching of BSA stabilized copper nanoclusters (BSA-CuNCs) in the presence of folic acid (FA). A. Fluorescence quenching of BSA-CuNCs at 644 nm when excited at 320 nm upon incremental addition of 2 µL of 1 mg/mL standard FA solution resulting in FA concentrations of 0, 0.67, 1.33, 2.00, 2.66, 3.32, 3.98, 4.64, 5.31, and 5.96 µg/mL (top to bottom, respectively) to a BSA-CuNCs solution (300 µg CuNCs in 3 mL). B. Plot of fluorescence intensity ratios versus FA concentration for the determination of LOD and LOQ. The LOD is 0.775 µg FA/mL, and the LOQ is 2.348 µg FA/mL.

Figure 3B shows a strong positive linear relationship (with correlation coefficient of 0.966) between folic acid concentration and the fluorescence quenching ratio, F_0/F with F_0 being the fluorescence intensity of the BSA-CuNCs without the quencher, while F refers to the new fluorescence intensity of the nanoclusters upon the addition of the quencher, folic acid, FA. The resulting Stern-Volmer equation is $F_0/F = 0.055[FA] + 1.026$, with the F_0/F dependent on the FA concentration [FA], with the slope or Stern-Volmer constant, K_{SV} at 0.055. The calculated figures of merit, limit of detection (LOD) and limit of quantification (LOQ) are shown in Table 1.

Table 1. Values from the Stern-Volmer plot for the determination the limits of detection (LOD) and quantification (LOQ) of folic acid using BSA copper nanoclusters as sensors.

PARAMETER	Values
Working range, µg/mL	2.348 – 5.964
Slope, Stern Volmer constant, K_{SV}	0.055
Standard deviation of slope	0.004
Intercept	1.026
Standard deviation of the intercept	0.013
Correlation coefficient (R^2)	0.966
Limit of detection (LOD), µg/mL	0.775
Limit of quantification (LOQ), µg/mL	2.348

The LOD and LOQ obtained were 0.775 µg/mL (1.756 µM) and 2.348 µg/mL (5.319 µM), respectively. The LOD was much higher in comparison to the LOD in other studies using copper nanoclusters (Table 2). Moreover, the working linear range of 2.348 – 5.964 µg/mL (5.319 to 13.511 µM) was narrower compared to published reports (Table 2). The current method seems to have lower sensitivity toward folic acid. Various factors that may have influenced sensitivity include instrument's calibration and sensitivity, and performance; methodological factors such as sensor and analyte preparations, solvent, temperature and pH; chemical factors such as matrix interference and analyte and sensor stability; sample and reagent quality; and human factors (Ellison and Hardcastle, 2012.)

Table 2. Comparison of figures of merit of fluorescence-based methods using copper nanoclusters for folic acid detection.

Nanomaterial	Method	Linear range	Limit of Detection	Reference
Beta-cyclodextrin-functionalized copper nanoclusters	Fluorescence quenching	4.95-47.6 μM	0.47 μM	Vegad et al., 2024
Ovalbumin-stabilized copper nanoclusters	Fluorescence quenching	0.5-200 μM	0.18 μM	Li et al., 2019
Double-stranded DNA (dsDNA)-templated copper nanoclusters (CuNCs)	Fluorescence quenching	1.25-50.00 μM	0.34 μM	Liu et al., 2023
Cysteine-CuNCs enhanced diperiodatoargentate(III) (DPA)-folic acid chemiluminescence	Fluorescence enhancement	0.10-10.00 μM	69.8 nM	Han et al., 2019
D-penicillamine (DPA)-stabilized Ag/Cu alloy nanoclusters	Fluorescence quenching	0.01 to 1200 μM	5.3 nM	Mei Zhang et al., 2024
Bovine serum albumin-copper nanoclusters (BSA-CuNCs)	Fluorescence quenching	2.348 – 5.964 μg/mL (5.319 to 13.511 μM)	0.775 μg/mL (1.756 μM)	This work

Table 3 shows the results of the determination of folic acid from four different over-the-counter supplements. The % errors of the experimental values compared to the declared content ranged from 33.31-40.21%. These error values are outside the acceptable precision error of 10% and acceptable accuracy error of 5% (Shrivastava et al., 2011). This may imply that the proposed method using the BSA-CuNCs may have some accuracy and precision issues.

Possible factors contributing to the % error values may include possible interferences from other components of the supplements, possible photodegradation of folic acid, possible losses during sample preparation, calibration and instrument errors. In the analysis of Cruces Blanco et al. (1994), fluorometric responses of derivatized folic acid using a labeling agent fluorescamine in the presence of Vitamins B1, B3, and B6 and minerals like iron, copper, zinc, phosphorus, calcium, fluorine, and iodine showed enhancement of fluorescence intensity due to possible fluorescence emission of the interfering compounds. In a study by Off et al. (2005), an increase in the fluorescence intensity of folic acid was observed when folic acid was exposed to UV radiation. The intact folic acid has a low quantum yield, so it gives a very weak fluorescence emission due to the possible quenching effect of its glutamyl tail. They attributed the increase in fluorescence to the cleavage of the C_9-N_{10} bond of the glutamyl tail, forming *p*-aminobenzoyl-L-glutamic acid and 6-formyl pterin.

Table 3. Folic acid (FA) determination in over-the-counter drugs using BSA-stabilized copper nanoclusters.

Sample/ Brand	Vol. of Solution, mL	DF	FA Content Declared	FA Content Experimental	SD	% Error	% Mean Recovery
A	100	20	5 mg	3.89 mg	1.29	33.31	77.75
B	100	20	5 mg	4.52 mg	1.75	38.81	90.31
C	100	20	5 mg	3.65 mg	1.27	34.90	72.94
D	100	10	600 mcg	396.01 mcg	159.25	40.21	66.00

n=11, DF-dilution factor, FA- folic acid, SD – standard deviation

Screening for Other Potential Analytes or Interfering Substances in Fluorescence-Based Sensing Using BSA-CuNCs. Aliquots of solutions of aluminum, arsenic, cadmium, mercury, molybdenum, lead, zinc, urea, and glucose were added to aqueous solutions of BSA-CuNCs to evaluate the emission responses of the BSA-CuNCs to substances besides folic acid (Figure 4).

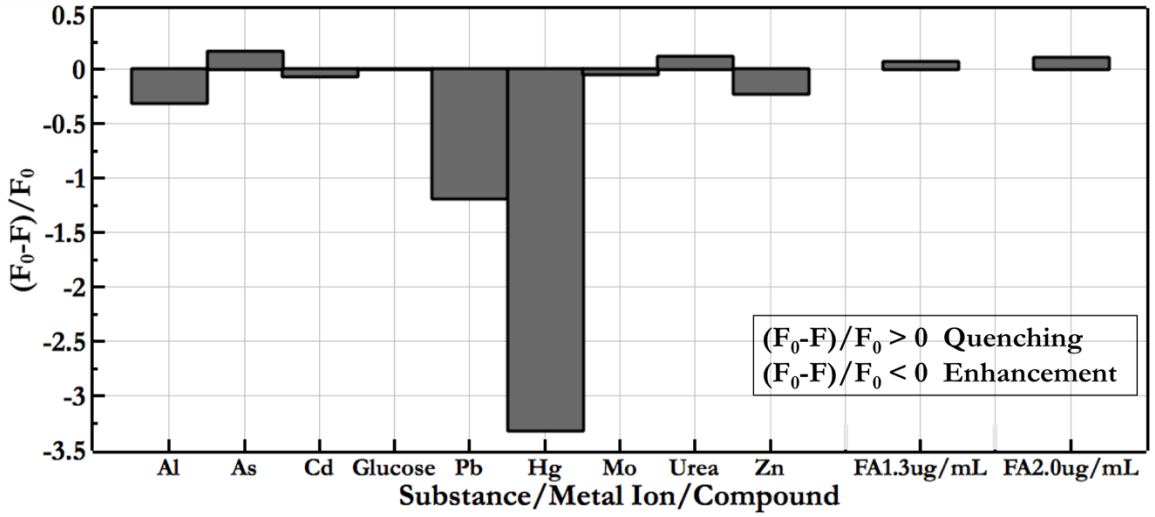

Figure 4. Fluorescence quenching or enhancement responses of the BSA stabilized copper nanoclusters at 644 nm excited at 320 nm when added with 1.5 ug/mL of various substances, metal ions or compounds. When the (F0-F)/F0, (where F0 is the fluorescence without the substance and F is the fluorescence with substance) is greater than zero, it indicates that the substance is a fluorescence quencher. When the (F0-F)/F0 is less than zero, the substance added is a fluorescence enhancer.

No significant change in fluorescence intensity was observed upon the addition of increasing amounts of glucose. This may imply that glucose may not affect the fluorescence of BSA-CuNCs, and may not cause interference during folic acid analysis.

Fluorescence quenching was observed when urea and arsenic were added. The quenching mechanisms may be similar when folic acid is present. For arsenic, the metal ion may have combined with the sulfhydryl groups on the surface of the nanoclusters, destroying the Cu-S bonds, which resulted in the fluorescence quenching (Xiaoqing et al., 2015). On the other hand, urea, may alter the BSA protein's structure (Stumpe and Grubmuller, 2007), thus affecting the stability of the CuNCs and possibly promote quenching of fluorescence.

There were some fluorescence enhancements in the presence of aluminum, cadmium, molybdenum, and zinc. The fluorescence enhancement was more pronounced in the presence of lead and mercury. Fluorescence enhancement may be due to various factors, as discussed by Li

et al. (2013). In this study, it may be hypothesized that such factors may include (1) formation of a complex between the metal ions and BSA; (2) reduction of the added metal ions by BSA or by ascorbic acid thus forming fluorescent species; (3) oxidation of the BSA or the CuNCs causing enhanced fluorescence; (4) interactions between the CuNCs and the reduced metal ions which can either change or not change the CuNCs composition; and (5) incorporation of reduced metal ions resulting to metal-CuNCs with enhanced fluorescence (Li et al., 2013).

These results showing that BSA-CuNCs had different responses to different substances may be useful for considering possible improvements in sample preparations or in exploring other potential analytes. These observations of fluorescence enhancement or quenching may have contributed to the lower-than-expected mean recoveries and relatively high standard deviation in the folic acid analysis in the supplement samples. Thus, the conditions in sample preparations for the fluorometric folic acid determination using the BSA-CuNCs must be optimized to achieve more accurate and precise results.

CONCLUSIONS

This study demonstrated the green synthesis of fluorescent BSA-stabilized copper nanoclusters (BSA-CuNCs) aided by ascorbate as a reducing agent. There seems to be some potential in the use of these BSA-CuNCs as sensors for the quantitative determination of folic acid in folic acid-containing supplements. However, more work should focus on solving potential issues on the selectivity and sensitivity towards the analyte, and on the sensors' responses toward the non-analyte components of samples.

ACKNOWLEDGMENTS

This work was supported by the UPLB Basic Research Program (Project ID 17855). The authors would like thank the UPLB Nanotechnology program and Dr. Yusuke Seto of the Kobe University, Department of Electrical and Electronic Engineering for the technical assistance.

REFERENCES

Aparna RS, Devi JA, Anjana RR, Nebu J, George S. Reversible fluorescence modulation of BSA stabilised copper nanoclusters for the selective detection of protamine and heparin. Analyst. 2019; 144(5):1799-808. https://doi.org/10.1039/C8AN01703D

Au L, Lim B, Colletti P, Jun Y, Xia Y. Synthesis of gold microplates using bovine serum albumin as a reductant and stabilizer. Chem Asian J. 2010 Jan 4; 5(1):123-129. https://doi.org/10.1002/asia.200900468

Blencowe H, Kancherla V, Moorthie S, Darlison M, Modell B. Estimates of global and regional prevalence of neural tube defects for 2015: a systematic analysis. Ann NY Acad Sci. 2018 Feb; 1414(1):31–46. https://doi.org/10.1111/nyas.13548

Chen Y, Chen C, Wang C, Liao W. Laminated copper nanocluster incorporated antioxidant paper device with rgb system-assisted signal improvement. Nanomaterials. 2018 Feb; 8(2):97. https://doi.org/10.3390/nano8020097

Cruces Blanco C, Segura Carretero A, Fernandez Gutierrez A, Roman Ceba M. Fluorometric determination of folic acid based on its reaction with the fluorogenic reagent fluorescamine. Anal Let. 1994 May; 27(7):1339-1353. https://doi.org/10.1080/00032719408006372

Ellison, SLR, and Hardcastle WA. Causes of error in analytical chemistry: results of a web-based survey of proficiency testing participants. Accreditation and Quality Assurance 17 (2012): 453-464. https://doi.org/10.1007/s00769-012-0894-2

Field MS, Stover PJ. Safety of folic acid. Annals of the New York Academy of Sciences. 2018 Feb; 1414(1):59-71. https://doi.org/10.1111/nyas.13499

Ghorbani H. Chemical synthesis of copper nanoparticles. Orient J Chem. 2014 Jun; 30(2):803-806. http://dx.doi.org/10.13005/ojc/300254

Glaubitz C, Rothen-Rutishauser B, Lattuada M, Balog S, Petri-Fink A. Designing the ultrasonic treatment of nanoparticle-dispersions via machine learning. Nanoscale. 2022 Sep; 14(35):12940–12950. PMCID: PMC9477382. https://doi.org/10.1039/D2NR03240F

Gokce Y, Cengiz B, Yildiz N, Calimli A, Aktas Z. Ultrasonication of chitosan nanoparticle suspension: Influence on particle size. Colloids and Surfaces A: Physicochemical and Engineering Aspects. 2014 Nov; 462:75–81. https://doi.org/10.1016/j.colsurfa.2014.08.028

Govindaraju S, Ankireddy S, Viswanath B, Kim J, Yun K. Fluorescent gold nanoclusters for selective detection of dopamine in cerebrospinal fluid. Sci Rep. 2017 Jan; 7:40298. https://doi.org/10.1038/srep40298

Hacisevki A. An overview of ascorbic acid biochemistry. J Fac Pharm Ankara. 2009 Sep; 38(3):233-255. https://doi.org/10.1501/Eczfak_0000000528

Han S, Chen X. Copper nanoclusters-enhanced chemiluminescence for folic acid and nitrite detection. Spectrochim Acta A: Mol Biomol Spectrosc. 2019 Mar; 210:315-320. https://doi.org/10.1016/j.saa.2018.11.051

Hemmateenejad B, Shakerizadeh-Shirazi F, Samari F. BSA-modified gold nanoclusters for sensing of folic acid. Sens Actuator B Chem. 2014 Aug; 199:42–46. https://doi.org/10.1016/j.snb.2014.03.075

Jain S, Nagar N, Devra V. Synthesis and characterization of highly efficient copper nanoparticles and their catalytic application in oxidative kinetic study. Adv Appl Sci Res. 2015; 6(6):171-180. https://www.primescholars.com/articles/synthesis-and-characterization-of-highly-efficient-copper-nanoparticles-andtheir-catalytic-application-in-oxidative-kinetic-study.pdf

Jardon-Maximino N, Perez-Alvarez M, Sirra-Avila R, Avila-Orta, C, Jimenez-Regalado E, Bello A, Gonzales-Morones P, Cadenas-Pliego G. Oxidation of copper nanoparticles protected with different coatings and stored under ambient conditions. J Nanomater. 2018 Sep; 9512768. https://doi.org/10.1155/2018/9512768

Jose L, Kuriakose S, Methew T. Bovine serum albumin stabilized silver nanoparticles: synthesis, characterization and antifungal studies. IOSR-JPBS. 2015 Jun; 10(3):19-25. Available from: https://iosrjournals.org/iosr-jpbs/papers/Vol10-issue3/Version-4/E010341925.pdf

Lerma-Garcia M, Avila M, Simo-Alfonso E, Rios A, Zougagh M. Synthesis of gold nanoparticles using phenolic acids and its application in catalysis. J Mater Environ Sci. 2014 Jul; 5(6):1919-1926. Available from: https://www.jmaterenvironsci.com/Document/vol5/vol5_N6/238-JMES-1305-2014-Lerma-Garcia.pdf

Li H, Yue Y, Liu T, Li D, Wu Y. Fluorescence-enhanced sensing mechanism of BSA-protected small gold-nanoclusters to silver(i) ions in aqueous solutions. J Phys Chem C. 2013 Jul; 117:16159-16165. http://dx.doi.org/10.1021/jp403466b

Li X, Wu X, Zhang F, Zhao B, Li Y. Label-free detection of folic acid using a sensitive fluorescent probe based on ovalbumin stabilized copper nanoclusters. Talanta. 2019 Apr; 195:372-80. https://doi.org/10.1016/j.talanta.2018.11.067

Liu L, Luo Y, Zhang X, Deng B, Zhen D, Zhou Z, Xie H, Liang H, Chen L. Rapid and sensitive determination of folic acid by facile synthesized dsDNA-CuNCs fluorescent probe. New J Chem. 2023 Sept; 47(39):18186-92. https://doi.org/10.1039/D3NJ02363J

Malvern Instrument Limited. [Internet]. Dynamic Light Scattering Common Terms Defined; 2011 [cited 2018 Nov 28]. Available from: http://www.biophysics.bioc.cam.ac.uk/wp-content/uploads/2011/02/DLS_Terms_defined_Malvern.pdf

Mei Zhang S, Xue Dong J, Li Wu X, Sen Zhao Y, Lei Li Y, Lin Wang S, Yang Y, An M, Su M, Ya Shi R, Feng Gao Z. A highly sensitive and selective fluorescent sensor for folic acid detection based on D-penicillamine stabilized Ag/Cu alloy nanoclusters. ChemBioChem. 2024 Jul; 25(14):e202400254. https://doi.org/10.1021/ac504520g

Mohd A, Khan A, Bano S, Siddiqi K. UV-absorption and fluorometric methods for the determination of alprazolam in pharmaceutical formulation. Arab J Chem. 2013 Oct; 6:369-378. http://dx.doi.org/10.1016/j.arabjc.2010.10.013

Nguyen VS, Rouxel D, Hadji R, Vincent B, Fort Y. Effect of ultrasonication and dispersion stability on the cluster size of alumina nanoscale particles in aqueous solutions. Ultrason Sonochem. 2011 Jan; 18(1):382–388. https://doi.org/10.1016/j.ultsonch.2010.07.003

Off MK, Steindal AE, Porojnicu AC, Juzeniene A, Vorobey A, Johnsson A, et al. Ultraviolet photodegradation of folic acid. J Photochem Photobiol B. 2005 Jul; 80(1):47–55. https://doi.org/10.1016/j.jphotobiol.2005.03.001

Ou G, Zhao J, Chen P, Xiong C, Dong F, Li B, et al. Fabrication and application of noble metal nanoclusters as optical sensors for toxic metal ions. Anal Bioanal Chem. 2018 Apr; 410(10):2485-2498. https://doi.org/10.1007/s00216-017-0808-6

Pacioni N, Filippenko V, Presseau N, Scaiano J. Oxidation of copper nanoparticles in water: mechanistic insights revealed by oxygen uptake and spectroscopic methods. Dalton Trans., 2013 Feb; 42:5832–5838. http://dx.doi.org/10.1039/c3dt32836h

Quinlivan EP, Hanson AD, Gregory JF. The analysis of folate and its metabolic precursors in biological samples. Analytical Biochemistry. 2006 Jan 15;348(2):163-84. https://doi.org/10.1016/j.ab.2005.09.017

Rahman T, Chowdhury M, Islam M, Akhtaruzzaman M. Microbiological assay of folic acid content in some selected Bangladeshi food stuffs. Int J Biol. 2015 Jan; 7(2):35-43. https://doi.org/10.5539/ijb.v7n2p35

Rajesh KM, Ajitha B, Ashok Kumar Reddy Y, Suneetha Y, Rreedhara Reddy P. Synthesis of copper nanoparticles and role of pH on particle size control. Mater Today Proc. 2016; 3(6):1985–1991. Available from: http://dx.doi.org/10.1016/j.matpr.2016.04.100

Santos L, Lecca R, Cortez-Escalante J, Sanchez M, Rodrigues H. Prevention of neural tube defects by the fortification of flour with folic acid: a population-based retrospective in Brazil. Bull World Health Organ. 2016 Jan; 94(1):22–29. https://doi.org/10.2471%2FBLT.14.151365

Selegard L. Synthesis, surface modification and characterization of metal oxide nanoparticles; nanoprobes for signal enhancement in biomedical imaging [dissertation]. [Sweden]: Linkoping

University Institute of Technology; 2013. 74 p. Available from: https://www.diva-portal.org/smash/get/diva2:619331/FULLTEXT01.pdf

Shrivastava A, Gupta V. Methods for the determination of limit of detection and limit of quantification of the analytical methods. Chron Young Sci. 2011 Jun; 2(1):21-25. https://doi.org/10.4103/2229-5186.79345

Singh A, Bandgar B, Kasture M, Prasad V, Sastry M. Synthesis of gold, silver and their alloy nanoparticles using bovine serum albumin as foaming and stabilizing agent. J Mater Chem. 2005 Dec; 15(48):5115–5121. http://dx.doi.org/10.1039/b510398c

Stumpe M, Grubmuller H. Interaction of urea with amino acids: implications for urea-induced protein denaturation. J Am Chem Soc. 2007 Dec; 129(51):16126-6131. https://doi.org/10.1021/ja076216j

Sun C. Size and confinement effect on nanostructures. ChemInform. 2006 May; 37(21):1-120. http://dx.doi.org/10.1002/chin.200621219

Teale F, Weber G. Ultraviolet fluorescence of the aromatic amino acids. Biochem J. 1957 Mar; 65(3):476–482. https://doi.org/10.1042%2Fbj0650476

Umavedi M. Fluorescence quenching by plasmonic silver nanoparticles. In: Geddes C. Surface plasmon enhanced, coupled and controlled fluorescence. 1st ed. John Wiley & Sons. 2017. p 197-202. Available from: http://dx.doi.org/10.1002/9781119325161.ch11

Vegad Y, Vardhan S, Ghosh AK, Jali BR, Sahoo SK. Folic Acid Detection Using β-Cyclodextrin-Functionalized Copper Nanoclusters and Vitamin B6 Cofactor Pyridoxal. ACS Applied Nano Materials. 2024 Feb; 7(4):4173-81. https://doi.org/10.1021/acsanm.3c05697

Qu X, Li Y, Li L, Wang Y, Liang J, Liang J. Fluorescent gold nanoclusters: synthesis and recent biological approach. J Nanomater. 2015 Aug; 6:1-23. https://doi.org/10.1155/2015/784097

Wang Y, Lihui H, Lingling L, Zhu J. Fluorescent gold nanoclusters: promising fluorescent probes for sensors and bioimaging. J Anal Test. 2017 Jun; 1:13. http://dx.doi.org/10.1007/s41664-017-0015-7

Xiaoqing L, Ruiyi L, Zaijun L, Xiulan S, Zhouping W, Junkang L. Fast synthesis of copper nanoclusters through the use of hydrogen peroxide additive and the application for fluorescent detection of Hg^{2+} in water samples. New J Chem. 2015 Apr; 39(7):5240-5248. http://dx.doi.org/10.1039/C5NJ00831J

Xie J, Zheng Y, Ying J. Protein-directed synthesis of highly fluorescent gold nanoclusters. J Am Chem Soc. 2009 Jan; 131(3): 888–889. https://doi.org/10.1021/ja806804u

Xiong J, Wang Y, Xue Q, Wu X. Synthesis of highly stable dispersions of nanosized copper particles using L-ascorbic acid. Geen Chem. 2011 Feb; 13:900-904. https://doi.org/10.1039/C0GC00772B

Xu J, Han B. 2016. Synthesis of protein-directed orange/red-emitting copper nanoclusters via hydroxylamine hydrochloride reduction approach and their application on Hg^{2+} sensing. NANO: Brief Rep Rev. 2016; 11(10):1650108. https://doi.org/10.1142/S1793292016501083

Zhao T, He X, Li W, Zhang Y. Transferrin-directed preparation of red-emitting copper nanoclusters for targeted imaging of transferrin receptor over-expressed cancer cells. J Mater Chem B. 2015 Jan; 3:2288-2394. https://doi.org/10.1039/C4TB02130D

Zheng J, Zhang C, Dickson R. Highly fluorescent, water-soluble, size-tunable gold quantum dots. Phys Rev Lett. 2004 Aug; 93(7):077402. https://doi.org/10.1103/physrevlett.93.077402